SWBSS2014
3rd International Conference on Salt Weathering of Buildings and Stone Sculptures
14-16 October 2014

The crystallization behavior of sodium magnesium sulfate in limestone

S. Godts*, R. Hendrickx and H. De Clercq
Royal Institute for Cultural Heritage (KIK-IRPA), Brussels, Belgium
* sebastiaan.godts@kikirpa.be

Abstract

The deterioration of porous building materials caused by single salts has been investigated extensively. Recently, more emphasis is given to the assessment of salt mixtures. Since a few years the ECOS/RUNSALT model is being used for the interpretation of the crystallization behavior of detected ion mixtures. The double salt bloedite or $Na_2Mg(SO_4)_2{\cdot}4H_2O$ is frequently found in the output of the predictive model. However, the crystallization behavior and the destructive effects of double salts such as bloedite are generally not documented. This paper presents the results of a research project carried out to assess the behavior of sodium magnesium sulfate in limestone related to that of the respective single salts. Limestone samples were contaminated with aqueous solutions of equimolar mixtures of sodium and magnesium sulfate at different concentrations and conditioned at different environmental conditions. The drying behavior as well as the crystallization behavior upon repeated drying-rewetting cycles was investigated. Identification of efflorescence was carried out by micro-Raman spectroscopy and XRD. The results indicate in general that the (initial) drying rate is an important factor for efflorescence development, which is influenced by ambient RH as well as the concentration of the salt solution used for the contamination of the samples. For samples contaminated with equimolar mixtures of Na_2SO_4—$MgSO_4$, konyaite $Na_2Mg(SO_4)_2.5H_2O$ precipitates during the first cycles, while only after several cycles bloedite $Na_2Mg(SO_4)_2{\cdot}4H_2O$ is identified.

Keywords: bloedite, konyaite, limestone, deterioration, conservation

1 Introduction

Damage to porous building materials and stone sculptures caused by the expansion pressures of salts is a well-known phenomenon, as described in a selective review by Doehne [1]. Over the past decade the thermodynamic ECOS/RUNSALT model [2], a mole-fraction-based model, is being used for the interpretation of the crystallization behavior of detected ion mixtures. The double salt bloedite or $Na_2Mg(SO_4)_2.4H_2O$ is frequently found in the output of the predictive model. However, the real behavior of the salt in practice or in lab is not documented.

This paper describes the results of the investigation on the crystallization behavior and damage potential of sodium magnesium sulfate on Maastricht limestone related to that of the respective single salts. The solution transport and drying behavior are investigated and compared to numerical calculations. The salt crystallization behavior in climatic conditions of 35 and 70% RH (25°C) is discussed.

2 Experimental procedure

Maastricht limestone samples are cut into 35 mm sided cubes. To avoid evaporation from the sides during absorption and drying, they are covered with sheets of dental modeling wax (Cavex®) applied with a heated spatula (Figure 1). The wax cover extends the height of the sample to avoid loss of efflorescence and to allow the addition of water during rewetting cycles.

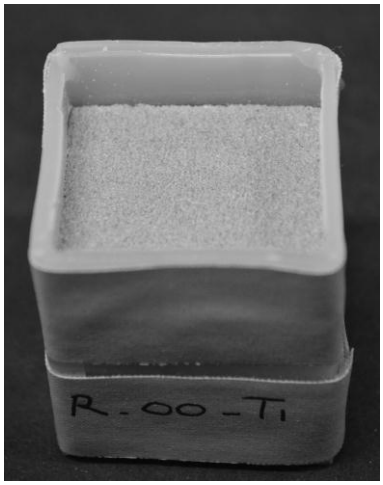

Figure 1: Sample with wax cover

Three sulfate concentrations are selected: 0.578, 1.100 and 1.700 mol/kg for a contamination with $MgSO_4$ and the equimolar mixture of Na_2SO_4 and $MgSO_4$. In case of Na_2SO_4, only the highest concentration (1.700 mol/kg) was tested as the lower ones have previously been investigated [3]. Per type of salt solution (7 in total), plus one reference test with pure water, four samples are used, which brings the total number of samples to 32.

Contamination was carried out by putting the bottom in contact with the salt solution or pure water. The capillary absorption rate was measured during the solution uptake, one sample per solution. Then, the bottom was closed off with transparent tape. Half of the samples (two of each group) were conditioned in a ventilated climate chamber at 35% RH and 25°C while the other half at 70% RH and 25°C to evaluate the drying behavior

and eventually the occurrence of damage over time upon repeated drying-rewetting cycles. The samples were weighed and photographed daily. After 14 days, an amount of water equal to the amount of evaporated water is poured on the top surface, dissolving all or most of the efflorescence. Consecutive rewetting and drying cycles are carried out (drying time of 14 days) until damage was visible. Due to practical circumstances the drying time of the sixth cycle was extended to 50 days. In total, 11 cycles were carried out. At the end of the program each sample was left to dry until constant weight was reached.

Efflorescence was identified with micro-Raman spectroscopy (Renishaw InVia). The measurements were carried out with a 780nm near infrared diode laser through a long-distance objective with a magnification of x5 or x50 reaching approximately 17,7 mW or 14,3 mW at the sample. An exposure time of 10 sec and a measurement range between 100.00 and 2000.00 cm^{-1} was sufficient to obtain identifiable spectra. At the end of the cycles the efflorescence is subjected to X-Ray Diffraction analysis (BRUKER D8 theta/2theta configuration).

3 Maastricht stone

Maastricht stone [4-6] is a pale yellow limestone, consisting mainly of microfossils and sand-sized fragments of microcrystalline carbonate. It is extremely light (density between 1300-1450 kg/m^3) and porous, has a low mechanical resistance (a compressive strength of 13.4-50 kg/cm^2), is easily scratched, and has a fine-grained, sandy structure. The microscopic structure resembles weakly cemented loose-packed sand. Because it is so easily workable and relatively frost resistant, it has been used frequently as a building stone in the Limburg region (Belgium and The Netherlands), especially during the Middle Ages and the Renaissance period.

The average porosity of the stone used for this investigation is 51%. The dominant pore size between 10 and 100 micron corresponds to the space between the grains. About 80% of the pore space corresponds to pores falling in this range, which means that the pore structure is highly monomodal. Some 20% of the pores (in volume) are smaller than 10 micron; this can be related to the intragranular porosity, like the hollows of fossils.

Because of its specific microstructure and properties, it is easily damaged by salts (fast and abundant uptake of solution and rapid drying). This has motivated researchers in Belgium and Europe to use it as a model material in lab experiments and it was also the reason why it was selected for the current test program.

The dry density of the Maastricht stone used in the tests is 1278±20 kg/m^3 (based on volume and measured dry mass). The average capillary water absorption coefficient derived from 5 measurements is 3.88±0.74

kg/m^{2}s$^{0.5}$ with an average capillary saturated water content (w_{cap}) of 418±18 kg/m³. This corresponds to a capillary saturation coefficient of (41.8/51.0)*100 = 82%. Due to the extremely fast absorption, it is not easy to measure the absorption rate because the process has to be interrupted at each measuring point. Apart from the intrinsic variations in the stone, this leads to a relatively important scatter in the results.

4 Results

4.1 Absorption and drying of limestone with salt solutions

The absorption rate of each of the salt solutions is expected to be equal to the one of water, scaled to the ratios of density and dynamic viscosity of the liquids. This was validated for very homogeneous materials [7-10], but not quantitatively for the Maastricht stone (Figure 2), although a trend of decreasing absorption rate (in volume units) and increasing saturation (in mass units; it remains approximately constant in volume units), was clearly observed for each case. One plausible explanation for this deviation is that the sharp front equation is an approximation and also that the increased surface tension, which leads to a higher capillary suction, was not accounted for. The theoretical approach is not further described in this paper.

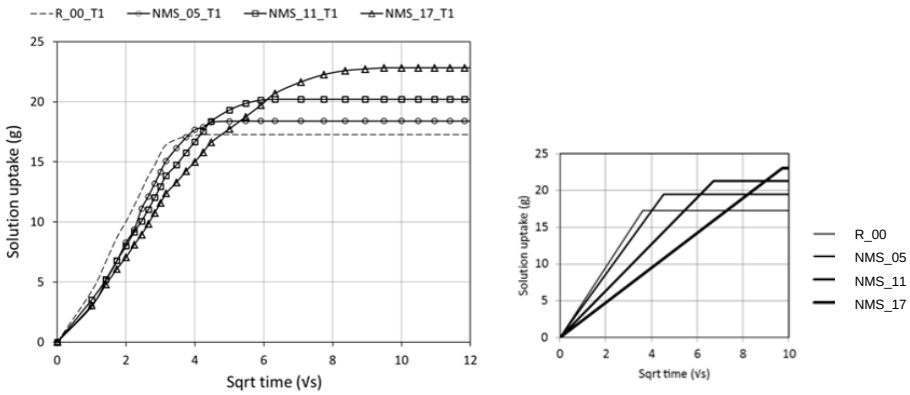

Figure 2: Absorption curves of one sample contaminated with sodium and magnesium sulphate in 3 concentrations and pure water, on the right the predicted curves. R: reference samples, NMS: sodium and magnesium sulfate, MS: magnesium sulfate in different concentrations 05: 0.578 mol/kg; 11: 1.100 mol/kg; 17: 1.700 mol/kg.

Drying of Maastricht stone with salts is expected to be slower than with water. The evaporation flux at the surface q_{evap} (kg/m^{2}s) is driven by the difference in vapor pressure at the surface ($p_{v,surf}$, Pa) and in the surrounding atmosphere ($p_{v,atm}$, Pa) and can be expressed by a simplified formula:

$$q_{evap} = \beta(p_{v,surf} - p_{v,atm})$$

with β a transfer coefficient which depends on the air flow pattern and the topography of the surface. In the case of pure water in the pores, the surface vapor pressure will remain equal to the saturation vapor pressure at the current temperature (RH 100%) as long as liquid water is transported to the surface from inside the stone.

Knowing that drying at 20°C and 50%RH leads to an initial rate of 0.42 kg/m²h for a vapor pressure difference of 2339-1169=1170 Pa in these test conditions, the expected initial drying rates for the salt solutions can be calculated (knowing the transfer coefficient β= 3.59e-4 h/m = 9.97e-8 s/m). It is assumed that liquid and gas phases are in equilibrium; i.e. the water activity (a_w) of the liquid phase equals the RH in the gaseous phase. The measured initial drying rates are an average over a period of the first 24 h. Although a substantial decrease of drying rate can already occur within 24h, for the sake of clarity and to keep the focus on the long-term effect, we kept the nomenclature of the "initial drying rate".

The experimentally measured initial drying rates are quite different from the calculated ones, and it appears that the difference can be related to the RH of the environment, the salt concentration and the type of salts introduced (Figure 3). A lower RH of 35% should theoretically lead to much faster drying. A trend in this sense could be observed, but not to the extent as could be expected theoretically. The lower-than-expected drying rates can be attributed to the blocking or clogging effect of crystallized salts near the surface, as was demonstrated for sodium chloride in brick by Gupta [11]. It was found that rapid drying (at little more than 0% RH) leads to the formation of "patchy" efflorescence, which tends to block the pores and prevents the formation of a receding drying front, while a slower drying leads to the formation of more protruding, cauliflower-shaped, "crusty" efflorescence that do conduct liquid. Eloukabi [12] also relates these two distinct drying regimes to the different types of efflorescence.

Similar remarks can be made on the effect of concentration: higher concentrations have systematically lower initial drying rates, but the effect is much stronger than expected and this deviation can again be attributed to clogging. Systematic trends according to the type of salt could not be observed from this analysis.

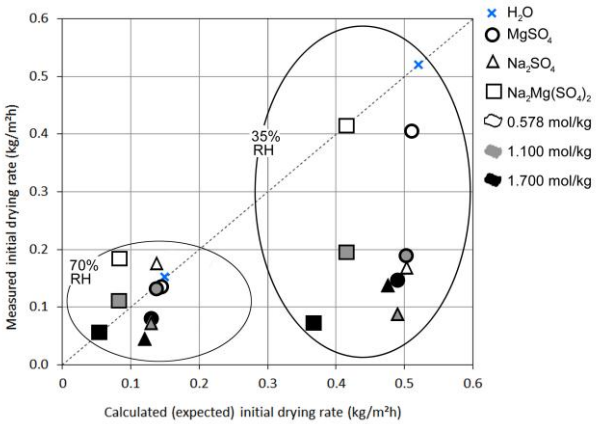

Figure 3: Experimentally measured (average of two samples) and calculated drying rates during the first 24 h after the uptake of salt solutions or pure water (1st cycle); the data are presented according to: the environmental RH (35 or 70 %) at 25°C, the molal concentration of the solutions, and the type of salt.

The experimentally measured initial drying rates (measured 24 hours after the start of each cycle) with pure water show a drying rate of about 0.52 kg/m²h for the samples conditioned at 35% RH and a lower rate of approximately 0.15 kg/m²h for the samples conditioned at a RH of 70%. The initial drying rate for the salt contaminated samples is generally lower compared to that of pure water (Figure 4). A significant drop of the drying rate occurs after the first cycle for the Maastricht stone contaminated with the lowest concentration of the equimolar mixture of sodium and magnesium sulfate (0.578 mol/kg) at 35% RH. There is a general trend of slower initial drying rates for all the samples during the first cycles, which stabilizes and then speeds up again after several cycles. This can be related to pore clogging and redistribution of salts after the addition of water at the start of each cycle.

Notable changes are observed over time when comparing the average evaporation rates over the last 24 h of each cycle (Figure 5). The water evaporation rate of the samples contaminated with magnesium sulfate in all three concentrations and those with 0.578 mol/kg sodium magnesium sulfate have is logically lower at higher RH. It becomes more complicated for the samples contaminated with a solution of 1.100 mol/kg as the evaporation rate dramatically increases after each cycle when conditioned at 70% RH, surpassing the evaporation rate of the samples conditioned at 35% (Figure 6). For the samples contaminated with a 1.700 mol/kg sodium magnesium sulfate solution this starts from the first cycle onwards. The increase of evaporated water at higher RH can be associated with a

decreased pore clogging, an increase in efflorescence and perhaps an increase in deterioration.

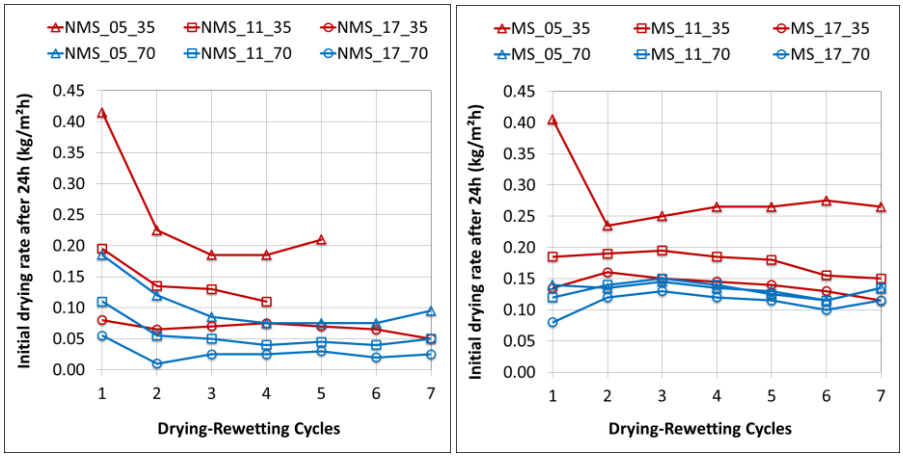

Figure 4: Average initial drying rate of samples contaminated with an equimolar mixture of sodium and magnesium sulfate (NMS, left) and magnesium sulfate (MS, right) in concentrations 0.578, 1.100 and 1.700 mol/kg) conditioned at 35 (red) and 70% (blue) RH (25°C) for each rewetting cycle.

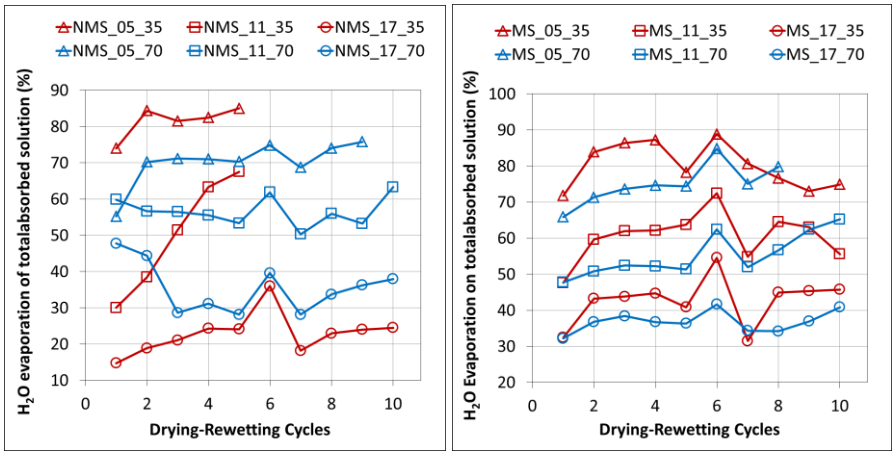

Figure 5: Evolution of the average evaporation of water (%) at the end of each cycle (after 14 days drying) except the 6th that ran over 50 days) of samples contaminated with sodium magnesium sulfate (NMS, left) and magnesium sulfate (MS, right) in different concentrations (05: 0.578 mol/kg ; 11: 1.100 mol/kg ; 17: 1.700 mol/kg) conditioned at 35 (red) and 70% (blue) RH (25°C).

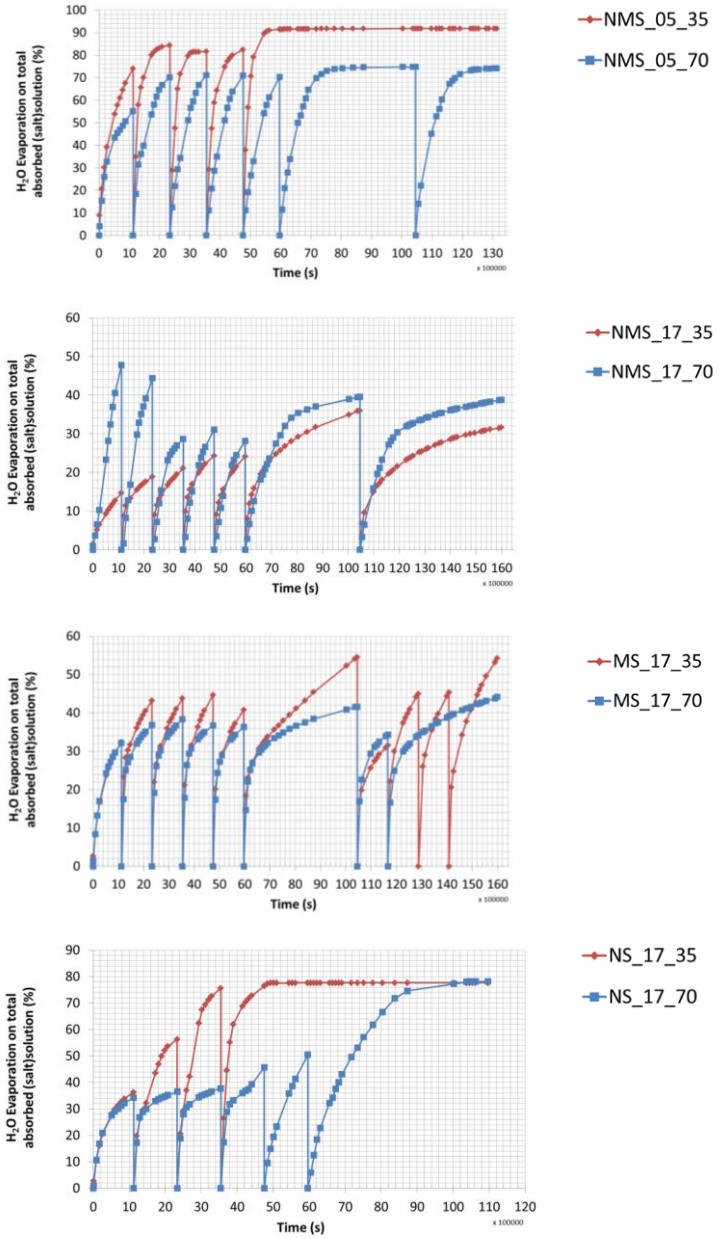

Figure 6: Average % evaporation of H_2O over time (sec) of two samples contaminated with sodium magnesium sulfate (NMS), magnesium sulfate (MS) or sodium sulfate (NS) at different concentrations (05: 0.578 mol/kg or 17: 1.700 mol/kg) at 35 (red) and 70% (blue) RH (25°C)

4.2 Salt crystallization processes

4.2.1 Evaporation properties and crystal growth

By observing the efflorescence deposit on the stone surface, significant differences are noticed (Figure 7). Where 35% RH generally leads to a rapid initial drying, patchy efflorescence develops (subsequently slowing down the process), a higher RH of 70% allows for slower but more sustained drying, leading to cauliflower-shaped efflorescence which doesn't block the moisture transport towards the evaporation face. Figure 7 illustrates this trend. Only the 2nd series from the top is an exception to this behavior as efflorescence develops on the surface of the samples at the lowest concentration of sodium magnesium sulfate. Apparently in this case at this stage the amount of salt is not sufficient to block the pores.

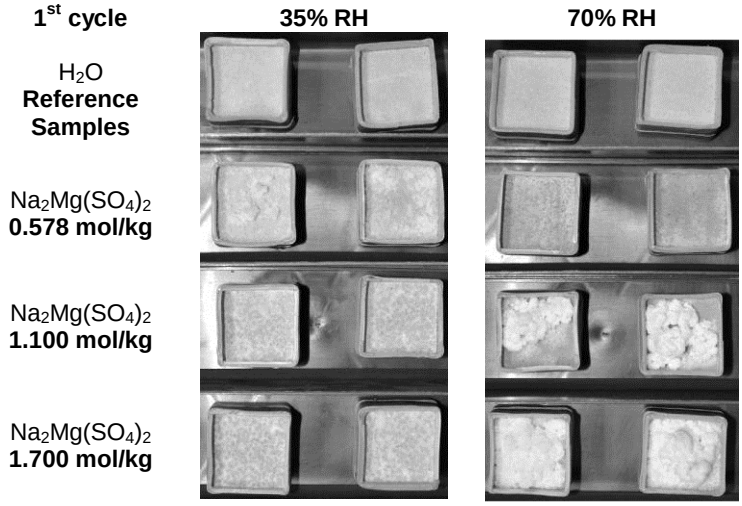

Figure 7: Images of the top faces of the specimens after 1 week of the 1st drying cycle at 35% RH (left) or 70% RH (right) at 25°C. Two specimens per case, contaminated with sodium magnesium sulfate in increasing concentrations from top (pure water) to bottom (1.700 mol/kg). Drying at high RH leads to cauliflower-shaped efflorescence, while low RH leads to efflorescence in patches.

After 1 week of the 2nd drying cycle at 35% RH, a decreasing amount of efflorescence for increasing salt concentration is observed (visually), while the opposite in case of a high RH (Figure 8). The explanation is the same: upon fast drying, a higher salt concentration leads to faster pore clogging

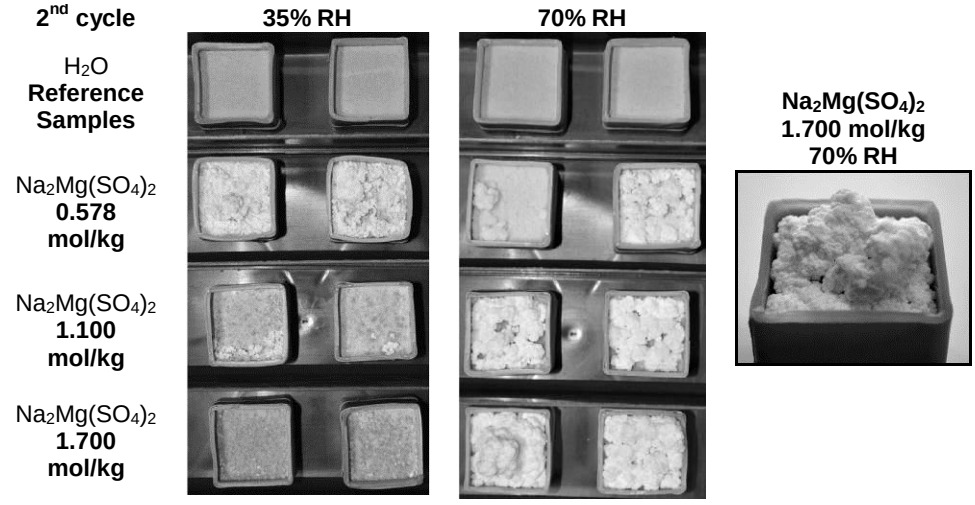

Figure 8: Image of the top faces of the specimens after 1 week of the 2nd drying cycle at 35% RH (left) or 70% RH (middle) at 25°C. Two specimens per case, contaminated with sodium magnesium sulfate in increasing concentrations from top (pure water) to bottom (1.700 mol/kg). Side view of a sample contaminated with sodium magnesium sulfate (1.100 mol/kg) conditioned at 70% RH (right).

This interpretation cannot be generalized to other types of salt. Figure 9 shows the top surfaces of the specimens contaminated with the single salts magnesium sulfate and sodium sulfate after one week of the 3rd cycle. Whereas the Maastricht stone is known for its rapid drying at the surface, magnesium sulfate is known for causing preferential subflorescence within limestone instead of efflorescence, when compared to sodium sulfate [13]. The higher viscosity of the magnesium sulfate solutions at equal molality, also decreasing the absorption rate, slows down their transportation (Table 1).

Sodium sulfate seems to be much less influenced by this pore clogging phenomenon: a drier environment leads to faster drying and more damage. The initial drying rate recorded in the first cycle is rather low (Figure 6) but increases a lot due to cracks formed, probably upon re-wetting in between the cycles.

Table 1: Solution Properties. Measurements obtained from: ■ Raf De Dier, Dept. of Applied Rheology, KULeuven, (viscometer Ubbelohde); ■ Michael Steiger, Dept. of Chemistry, UHamburg; ■ CRC Handbook interpolated; ■ Estimated based on ratio eta25/eta20 of $MgSO_4$; ■ Wikipedia

	Na_2SO_4			$MgSO_4$			$Na_2Mg(SO_4)_2$			H_2O
mol/kg	0.578	1.100	1.700	0.578	1.100	1.700	0.578	1.100	1.700	
density at 25°C (kg/l)	1.066	1.123	1.183	1.064	1.120	1.182	1.127	1.229	1.331	0.997
kinematic viscosity at 25°C (mm^2/s)				1.226	1.634	2.367	1.246	2.497	4.832	0.901
dynamic viscosity at 25°C (mPas)	1.104	1.418	1.904	1.304	1.831	2.797	1.405	3.069	6.431	0.898
density at 20°C (kg/l)	1.067	1.152	1.185	1.066	1.122	1.183				0.998
kinematic viscosity at 20°C (mm^2/s)				1.382	1.860	2.689	1.667	2.860		1.026
dynamic viscosity at 20°C (mPas)	1.255	1.611	2.164	1.473	2.087	3.182				1.002

During the 9th cycle at 35% RH efflorescence is still not visible on the top face of the samples contaminated with magnesium sulfate at all concentrations (Figure 10). The surface of the samples contaminated with the lowest concentration starts to bulge. By the end of the test when the wax around the samples is removed, as shown in figure 10, it becomes clear that sub-florescence has deteriorated a superficial layer of approximately 3mm thickness.

At 70% RH a decreasing amount of efflorescence for increasing salt concentration is noticed, in contrary with the results obtained for sodium magnesium sulfate. The explanation is the same in both dry and moist conditions: upon drying, a higher salt concentration leads to faster pore clogging. The discrepancy compared to the sulfate mixtures can be caused by the higher viscosity of the magnesium sulfate solutions (Table 1).

Further evidence is found in the earlier plotted drying rates (Figure 3). It shows that the highest concentration reduces significantly the drying rate compared to the lower concentrations, and that magnesium sulfate tends to cause a further reduced decrease of the expected initial drying rate when compared to sodium sulfate and the sulfate mixture (Figure 6).

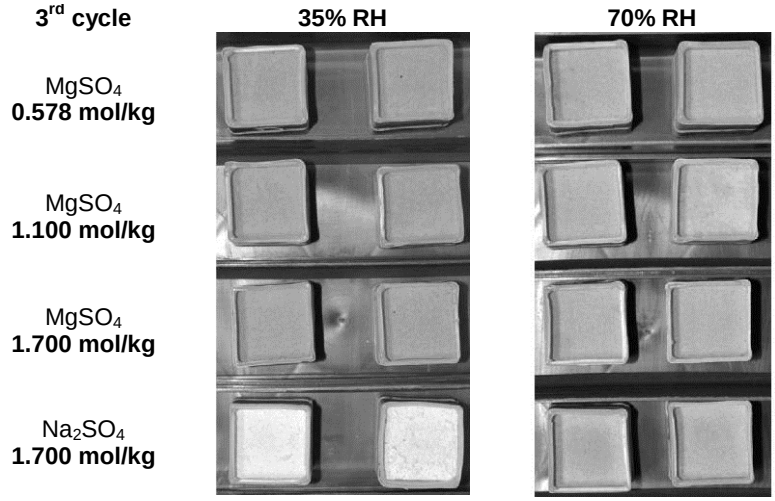

Figure 9: Photograph of the top faces of the specimens after 1 week of the 3rd drying cycle at 35% RH (left) or 70% RH (right) (25°C). Two specimens per case, contaminated with, from top to bottom, magnesium sulfate in increasing concentrations starting from 0.578 to 1.700 mol/kg or sodium sulfate (1.700 mol/kg).

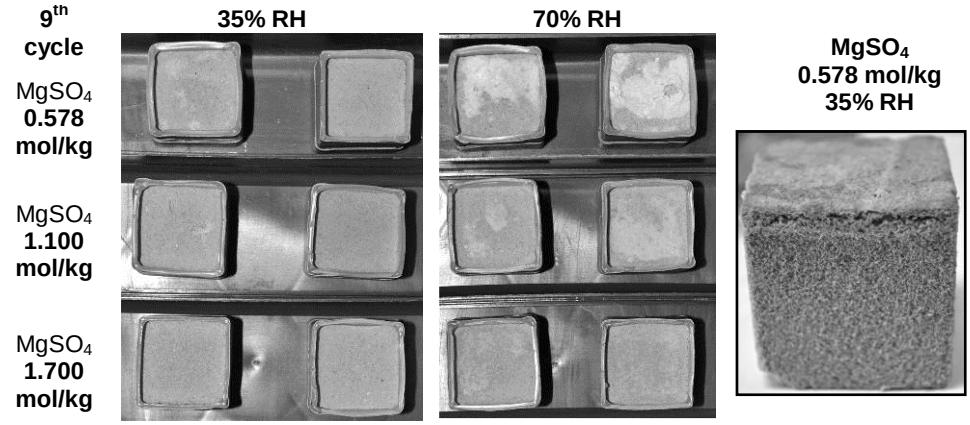

Figure 10: Photograph of the top faces of the specimens after 1 week of the 9th drying cycle at 35% RH (left) or 70% RH (middle) at 25°C. Two specimens per case, contaminated with magnesium sulfate in increasing concentrations starting from top (0.578 mol/kg) to bottom (1.700 mol/kg). Side view of a sample contaminated with magnesium sulfate (0.578 mol/kg) conditioned at 35% RH (right).

4.2.2 Identification of efflorescence

Efflorescence on the samples is investigated with Raman spectroscopy during the second week of each cycle. An average of five measurements is systematically carried out each time efflorescence is visible on the top face. When efflorescence with a different morphology is observed under the microscope, it is also investigated. The obtained spectra are identified with reference spectra obtained from [14] (Table 2). Five main spectra were identified during the entire program (Figure 11). The Raman spectrum of konyaite shows in the range of 900-1100 cm^{-1} a double band at 983.2 and 1005.3 cm^{-1}, while that for bloedite shows only one band at 992.1 cm^{-1}. The efflorescence of samples contaminated with 0.578 mol/kg of Na_2SO_4—$MgSO_4$ conditioned at 70% RH show one strong band at 980.4 cm^{-1} that could not be attributed to a particular phase (Figure 11).

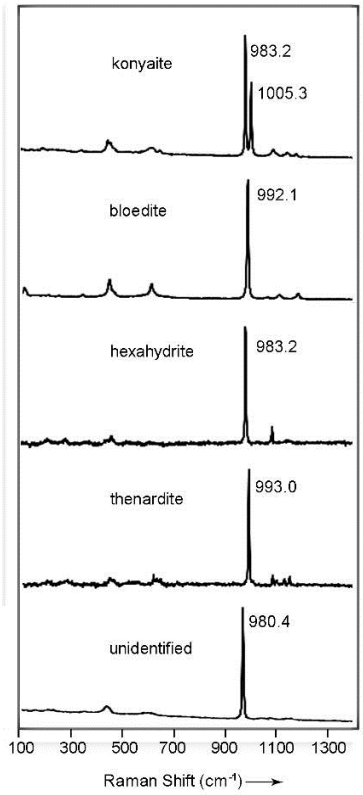

Figure 11: Raman spectra of the efflorescence

The results show that for all the samples containing equimolar mixtures of Na_2SO_4—$MgSO_4$ at all tested concentrations, only konyaite or $Na_2Mg(SO_4)_2.5H_2O$ effloresces during the first cycles (Table 3) while bloedite or $Na_2Mg(SO_4)_2.4H_2O$ later on. Both double salts bloedite and konyaite are analyzed by XRD at the end of the cycles.

For the samples contaminated with $MgSO_4$ only sub-florescence is visibly clogging the pores at the surface of all the samples conditioned at 35% RH with a rare exception for the highest concentration. In case of increased RH, almost no efflorescence is visible on the top face until the 5th cycle with an exception of the samples contaminated with a solution of 1.100 and 1.700 mol/kg of $MgSO_4$. Only after the longer 6th cycle efflorescence becomes visible on all the samples conditioned at 70% RH.

The Raman spectra revealed the crystallization of hexahydrite (983.2 cm^{-1}). Although the main band of it is quite close to that of $MgSO_4.7H_2O$ (984.5 cm^{-1}), and hence not easy to distinguish, XRD confirmed the presence of hexahydrite. As expected the efflorescence on the samples containing Na_2SO_4 consists of thenardite (Raman band at 993.0 cm^{-1}), further confirmed by XRD at the end of the program.

Table 2: Main Raman bands (cm^{-1}) of the identified efflorescence compared to the reference spectra and literature

	Measured	Reference spectra [14]	[15]	[16]
Konyaite	983.2	983.5	981	—
	1005.3	1005.5	1003	
Bloedite	992.1	992.0	995	—
Hexahydrite	983.2	983.0	—	983.6
Epsomite	—	984.5	—	984.1
Thenardite	993.0	993.0	—	—

Table 3: Identification of salt efflorescence with micro-Raman spectroscopy during the second week of each cycle and identification with XRD at the end of the program. The samples for which bloedite was detected are marked in gray.

sample / cycle	C1	C2	C3	C4	C5	C6	C7	C8	C9	C10	C11
NMS_05_35	K	K	K	K	K	K/B	K/B	K/B	K/B	K/B	K/B (X)
NMS_05_70	U	K/U	K	K	K/B	K	K/U	K/B	K/B	K/B	K/B (X)
NMS_11_35	K	K	K	K	K	K/B	K/B	K/B	K/B	K/B	K/B (X)
NMS_11_70	K	K	K	K	K	K	K/B	K/B	K/B	K/B	K/B (X)
NMS_17_35	K	K	K	K	K	K/B	K/B	K/B	K/B	K/B	
NMS_17_70	K	K	K/B	K/B	K/B	K/B	K/B	K/B	K/B	K/B	
MS_05_35						S	S	S	S	S	
MS_05_70						H	H	H	H	H	H (X)
MS_11_35						S	S	S	S	S	
MS_11_70		H	H	H	H	H	H	H	H	H	
MS_17_35					H	H	S	S	S	S	
MS_17_70	H					H	H	H	H	H	
NS_17_35		T	T	T	T	T	T	T	T	T	T (X)
NS_17_70	T			T	T	T	T	T	T	T	T (X)

Legend:
NMS: $Na_2Mg(SO_4)_2$
MS: $MgSO_4$
NS: Na_2SO_4
05: 0.578 mol/kg
11: 1.100 mol/kg
17: 1.700 mol/kg
35: 35% RH, 25°C
70: 70% RH, 25°C
C: cycle number
K: konyaite
B: bloedite
U: unidentified
S: sub-florescence
H: hexahydrite
E: epsomite
T: thenardite
(X): XRD

5 Conclusions

The absorption rate of each of the sulfate solutions in the experiments with the Maastricht stone did not correspond to the expected rates. However, the decreased absorption and increased saturation compared to pure water remain rather constant for each case. The results show significant differences in drying behavior between the individual salts and the salt mixture, between different concentrations and RH conditions. Important deviations were found for drying at the lower RH: a fast initial drying leads to pore clogging in almost all cases, subsequently slowing

down the process. This confirms previous studies which stated that, for salts which are prone to pore clogging, high RH drying appears more effective because it reduces the clogging effect. The preliminary observations on the damage potential of the single salts Na_2SO_4 and $MgSO_4$ are generally in agreement with recent literature [13, 17].

In general it can be concluded that a lower concentration and a lower RH leads to higher amounts of efflorescence deposited at the surface of samples contaminated with Na_2SO_4—$MgSO_4$ while higher concentrations tend to lead to a stronger pore clogging reducing efflorescence, and vice versa at a higher RH. This phenomenon can also be concluded for samples contaminated with the single salt $MgSO_4$ with an important discrepancy in case of more humid conditions where higher concentrations also tend to lead to a stronger pore clogging and a reduced efflorescence.

The Na_2SO_4 contaminated samples dry fast and large amounts of thenardite sub- and efflorescence are produced causing rapid deterioration and layer detachment, which is first observed for the samples conditioned at 35% RH. $MgSO_4$ contaminated samples dry slower; damage is mainly caused by hexahydrite subflorescence causing bulging, followed by the collapse of the surface layer, probably occurring during rewetting. The subflorescence causes internal crack formation after a significant amount of cycles, which is first detected for the samples conditioned at 70% RH while only later at 35%. For samples contaminated with an equimolar mixture of sodium and magnesium sulfate, konyaite or $Na_2Mg(SO_4)_2{\cdot}5H_2O$ precipitates during the first cycles, while only after several cycles bloedite $Na_2Mg(SO_4)_2{\cdot}4H_2O$ crystallized, although frequently appearing in the output of ECOS/RUNSALT.

From this investigation it can be concluded that the salt crystallization behavior depends on the cycle numbers. In order to understand the behavior of double salts the execution of a sufficient amount of crystallization cycles is crucial. In general we can state that the (initial) drying rate is an important factor for the damage potential, which is influenced by the ambient RH as well as the salt type and concentration of the solution. A lower concentration leads to a higher damage potential in samples contaminated with $Na_2Mg(SO_4)_2$. Again, this can be explained by the stronger pore clogging effect when using higher concentrations. Furthermore, the preliminary results indicate that the formation of bloedite possibly causes a further decrease in the drying rate perhaps due to its less soluble nature compared to konyaite.

References

[1] E. Doehne. Salt weathering: a selective review. In: Natural Stone, Weathering Phenomena, Conservation Strategies and Case Studies: Edited by S. Siegesmund, T. Weiss and A, Vollbrecht - Geological Society of London, (2002)

[2] C. Price (Ed.). An expert chemical model for determining the environmental conditions needed to prevent salt damage in porous materials. European Commission Research Report No 11, (Protection and Conservation of European Cultural Heritage). London: Archetype Publications, (2000)

[3] H. De Clercq, M. Jovanović, K. Linnow, M. Steiger. Performance of limestones laden with mixed salt solutions of Na_2SO_4–$NaNO_3$ and Na_2SO_4–K_2SO_4, Environmental earth sciences, 69 (5), (2013), pp 1751-1761

[4] CW. Dubelaar, M. Dusar, R. Dreesen, WM. Felder, TG. Nijland. Maastricht limestone: a regionally significant building stone in Belgium and the Netherlands. Extremely weak, yet time-resistant. In Fort R, de Buergo MA, Gomez-Heras M and Vazquez-Calvo C (eds): Proceedings of the International Heritage, Weathering and Conservation Conference, Taylor&Francis Group, London, (2006), pp 9-14

[5] E. Roekens, E. Leysen, E. Stulens, J. Philippaerts, R. Van Grieken. Weathering of Maastricht Limestone Used in the Construction of Historical Buildings in Limburg, Belgium. In Ciabach J (ed): Proceedings of the 6th International Congress on Deterioration and Conservation of Stone, Nicholas Copernicus University Press Department, Torun, (1988), pp 45-56

[6] M. Dusar, R. Dreesen, A. De Naeyer. Renovatie & Restauratie, Natuursteen in Vlaanderen, versteend verleden. Wolters Kluwer België NV, (2009), pp 427-437

[7] R. Hendrickx, S. Roels, H. De Clercq, Y. Vanhellemont. Experimental Determination of Liquid Transport Properties on Salt-Contaminated Porous Stone. In V. De Freitas, H. Crovacho, & M. Lacasse (Eds.), 12th International Conference on Durability of Building Materials and Components, Porto, 12-15 April 2011, Rotterdam (2011), pp 125–132

[8] H. Derluyn, M. Griffa, D. Mannes, I. Jerjen, J. Dewanckele, P. Vontobel, A. Sheppard, D. Derome, V. Cnudde, E. Lehmann, J. Carmeliet. Characterizing saline uptake and salt distributions in porous limestone with neutron radiography and X-ray micro-tomography, Journal of Building Physics, 36 (4), (2013), pp 353–374, doi:10.1177/1744259112473947

[9] C. Hall, WD. Hoff. Water transport in brick, stone and concrete. London: Taylor & Francis, (2002)

[10] AS. Poupeleer. Transport and crystallization of dissolved salts in cracked porous building materials. PhD thesis KU Leuven, (2007)

[11] S. Gupta. Sodium chloride crystallization in drying porous media: influence of inhibitor. PhD thesis Eindhoven University of Technology, (2013)

[12] H. Eloukabi, N. Sghaier, S. Ben Nasrallah, M. Prat. Experimental study of the effect of sodium chloride on drying of porous media: The crusty–patchy efflorescence transition, International Journal of Heat and Mass Transfer, 56 (1-2), (2013), pp 80–93

[13] A. Ruiz-Agudo, F. Mees., P. Jacobs, C. Rodriguez-Navarro. The role of saline solution properties on porous limestone salt weathering by magnesium and sodium sulfates. Environ Geol (52), (2007), pp 269-281

[14] Reference spectra obtained from Kirsten Linnow and Nadine Lindstroem, University of Hamburg, Department of Chemistry, Inorganic and Applied Chemistry, Michael Steiger Research Group.

[15] P. Vargas Jentzsch, B. Kampe, P. Rösch, J. Popp. Raman Spectroscopic Study of Crystallization from Solutions Containing $MgSO_4$ and Na_2SO_4: Raman Spectra of Double Salts, The Journal of Physical Chemistry 115 (22), (2011), pp 5540-5546

[16] A. Wang, JJ. Freeman, BL. Jolliff, IM. Chou. Sulfates on Mars: A systematic Raman spectroscopic study of hydration states of magnesium sulfates. Geochimica et Cosmochimica Acta 70, (2006), pp 6118-6135

[17] M. Steiger, K. Linnow, H. Juling, G. Gülker, A. El Jarad, S. Brüggerhoff, D. Kirchner. Hydration of $MgSO_4.H_2O$ and generation of stress in porous materials. Crystal Growth & Design 8 (1), (2008), pp 336–343